Scientific Research Publishing

World Journal of Engineering and Technology, 2016, 4, 174-185
http://www.scirp.org/journal/wjet
ISSN Online: 2331-4249
ISSN Print: 2331-4222

XRD Doping Control of Light-Emitting cBN with a Large Size Mismatch between the Dopant and Intrinsic Atoms

E. M. Shishonok[1], V. G. Luhin[1], J. W. Steeds[2]

[1]Belarusian State University of Technology, Minsk, Republic of Belarus
[2]School of Physics, University of Bristol, Bristol, UK
Email: eshishonok@tut.by

How to cite this paper: Shishonok, E.M., Luhin, V.G. and Steeds, J.W. (2016) XRD Doping Control of Light-Emitting cBN with a Large Size Mismatch between the Dopant and Intrinsic Atoms. *World Journal of Engineering and Technology*, **4**, 174-185.
http://dx.doi.org/10.4236/wjet.2016.43D021

Received: September 19, 2016
Accepted: October 13, 2016
Published: October 20, 2016

Abstract

Cubic boron nitride (cBN) as the outstanding representative of the family of semiconducting wide bandgap nitrides and the closest analogue of diamond, is produced and investigated. XRD as method for doping control of cBN with impurities of large atomic sizes, is suggested. The larger an atomic size mismatch between doping and intrinsic atoms of a semiconductor's crystal lattice, the stronger its response through own strains and distortions. The distortions are expected to be notable in the case of the smallest intrinsic atoms of cBN and diamond. The light-emitting cBN doped with various rare-earth elements (RE) in different concentrations under high pressure conditions is synthesized in form of the cBN: RE single phase micropowders. The micropowders showed the discrete photoluminescence spectra in IR-, red and green spectral ranges which were attributed to the intra-electronic transitions of RE^{3+} ions located in cBN crystal lattice. The locations of the RE^{3+} ions in cBN crystal lattice are discussed. The data of XRD ($Cu_{K\alpha}$) analysis of the cBN:RE micropowders are represented. Extra-splits (as the additional ones to the α_1-α_2-splits on $Cu_{K\alpha}$) of the cBN parent peaks in XRD patterns of the cBN: RE, are discovered and analyzed using appropriate computer programs. As established, crystal lattice of cBN due to the incorporation of RE^{3+} ions, represents a disordered solid solutions which are nonuniformly distorted in dependence on the ions' size and their concentrations in cBN. Results of the present work can be useful to manufacture cBN with predictable functional properties, as well as for in situ doping control of cBN and diamond.

Keywords

Cubic Boron Nitride, High Pressure, Rare Earth Element, İon, Concentration, Photoluminescence, XRD Analysis, Crystalline Distortion

1. Introduction

Cubic boron nitride (cBN) is the widest bandgap (E_g = 6.4 eV) semiconductor in the AIIIBV group. CBN is the closest analog of diamond but is superior to the latter in the bandgap width, thermal, radiation, and chemical stability, the possibility of forming n- and p-type conduction, and the capability of emitting secondary electrons. CBN has been recognized as the unique material promising for the use in opto- and microelectronics, including for the employment in light emitters of various purposes operative in UV, visible, and IR spectral regions. Understandably, the successful production of RE-activated cBN samples exhibiting intense light emission in the IR, visible, and UV spectral ranges, variously stimulated, might open up opportunities for manufacturing new generation light-emitting diodes, solid state lasers, detectors, and phosphors operating under extreme conditions. Rigidity of the crystal lattice of cBN will ensure mechanical strength, radiation stability, and the capability of operating under the conditions of high electric fields for all devices based on cBN. It is expected that the high thermal stability will make cBN virtually indispensable for the use in passive elements of future electron devices, such as takeoffs of heat from chips with high heat release, by ensuring their high operation speed. A high speed of sound will make it possible to use cBN in devices operating in a gigacycle range, and the presence of piezoelectric properties will allow its employment in piezo elements, under extreme operational conditions. At last, cBN has been announced as promising functional material for future quantum computers [1]. Among the main reasons for slow "mastering" of cBN as a functional material for solid state electronics is the absence of large perfect single crystals of cBN. On the other hand, a good alternative to single crystals of cBN for opto- and microelectronic applications can be its other morphological forms, like micropowders which, while exhibiting intense light emission (LE) are ready for the utilization by downconversion phosphors.

2. Experimental Details

The cBN:RE (RE: rare earth element) yellow micropowders were manufactured under high pressure-high temperature (HPHT) via catalytic synthesis from hBN in presence of the low-melting compound based on RE (Er, Tb, Eu, Sm, Nd). The granulometric analysis of cBN:RE micropowders was provided with "Laser particle size analyzer LS-POP(VI), OMEC INSTRUMENTS CO., LTD". For all micropowders', *the volume mean diameters* D(4,3) ≈ 3.5 - 5.5 μm of grains, were revealed. The grains enlarged in size were observed, when the concentrations of the RE largest ions in cBN increased. CBN micropowders were analyzed in their phase content using XPS and RBS methods, which data coincided well. If the precursors of cBN contained 0.5 - 15 wt. % of the RE compound, only from less than 0.01 up to ~0.1 at. % of the RE element could be introduced into crystal lattice of cBN using the concrete catalytic system. XRD patterns of the micropowders were taken repeatedly with recording step of 0.01˚/min using D8 Advance Bruker AXS instrument on $Cu_{K\acute{a}}$ radiation. For measurements, the equal masses of the micropowders were placed into standard cuvettes. The rotation option of

samples was not used, because of small sizes of the micropowders' grains. Computer programs were used for deconvolution of the XRD patterns' peaks on the minimal number of components, a package of which gave calculated peaks with the ~5% deviation from the experimental peaks. It was taken into account that the ratio of intensities of $\acute{\alpha}_1$- and $\acute{\alpha}_2$-component in $Cu_{K\alpha}$-doublet is equal almost two and the components have the equal half-widths. The contributions of a Lorentzian and a Gaussian into an experimental peak's shape, which both cause either the particle-size broadening or the instrumental and strain-broadening of the peak correspondingly, allowed us to use the Voigt profiles as a natural description of peaks in XRD patterns of the cBN:RE micropowders.

Generally, photoluminescence (PL) tests of cBN:RE were performed using RENISHAW-1000 spectrometers at room temperature.

3. Results and Discussion

3.1. Photoluminescence Testing

The PL discrete spectra (λ_{exc} = 488 nm) of cBN:Eu micropowders with ~0.01, ~0.05 and 0.1 at.% Eu in cBN are represented in **Figures 1(a)-(c)**. They are originated from the consequence of the radiative electronic transitions $^5D_0 \rightarrow {}^7D_J$ (J = 0, 1, 2, 3, 4) of Eu^{3+} ions which are located in cBN crystal lattice in crystalline field of low symmetry [2]. In this work we first can obtain, that headlines of the spectra (the insets in **Figures 1(a)-(c)**) are visibly split into two separate main lines. It means that Eu^{3+} ions occupy two sites of

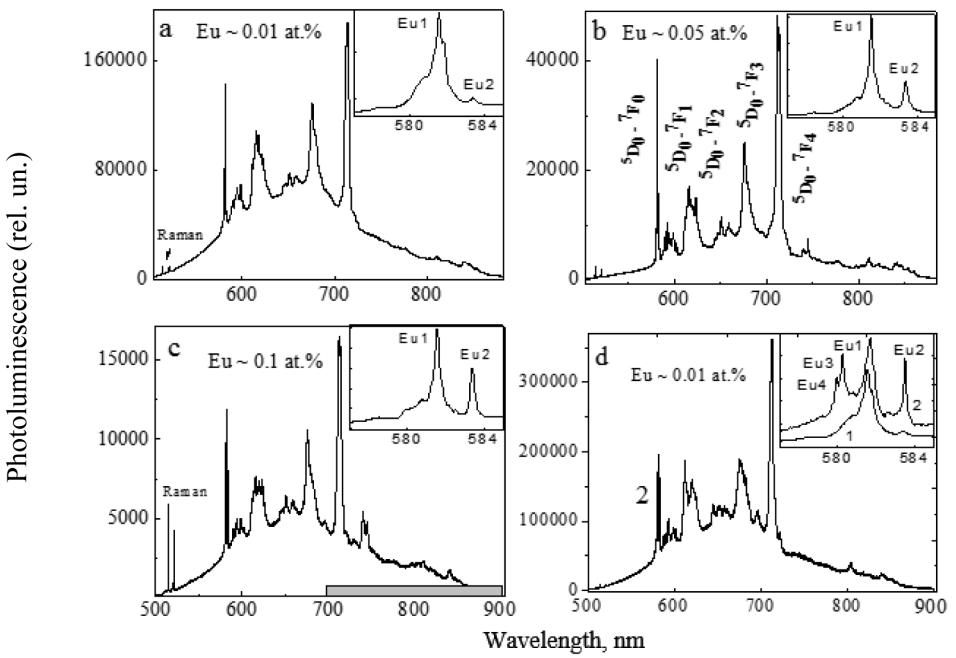

Figure 1. PL spectra of cBN:Eu micropowders with different Eu content in cBN: ~0.01 (a), ~0.05 (b) и ~0.1 at.% (c), and of cBN:Eu (~0.01 at.% Eu) before (1) and after annealing at T_{ann} = 870 K (2) (d) in the inset; λ_{exc} = 488 nm, T_{reg} = 300 K.

low symmetry in the cBN crystal lattice which create two luminescence centers (we called them Eu1 and Eu2). It is clear from the insets, that the Eu^{3+} ions occupy the second site in cBN crystal lattice the more expectable, the more concentration of Eu in cBN. The two-center character of Eu in cBN was suggested in our previous work [3]. The represented data here directly testify to the suggestion. The Eu1 and Eu2 centers have already figured in [3], but they were observed among four luminescence centers in PL spectra of the cBN:Eu (~0.01 at.% Eu) micropowder which was annealed at T_{ann} = 870 K (**Figure 1(d)**, the inset). More likely, that the annealing effect is caused by redistribution of Eu^{3+} ions among sites in cBN crystal lattice due to activation in it of the nitrogen vacancies' motion [4]. The PL multiband spectra (λ_{exc} = 488 nm) of cBN:Tb micropowders (**Figure 2(a)** and the inset) are related here to the $^5D_4 \rightarrow {}^7F_{6,5,4,3}$ intra-electronic transitions of Tb^{3+} ions. The cBN:Tb spectrum considerably increases in intensity when the Tb concentration in cBN grows from ~0.05 up to ~0.1 at. %. In this case, the spectrum remains structurally unchanged. It meant, that Tb^{3+} ions continue locating in the similar crystallographic positions inside cBN crystal lattice. The ions stay in the same positions after annealing the cBN:Tb (0.1 at.% Tb) at T_{ann} = 870 K, in opposite to the annealed cBN:Eu (**Figure 1(d)**). However, the PL spectrum of the annealed

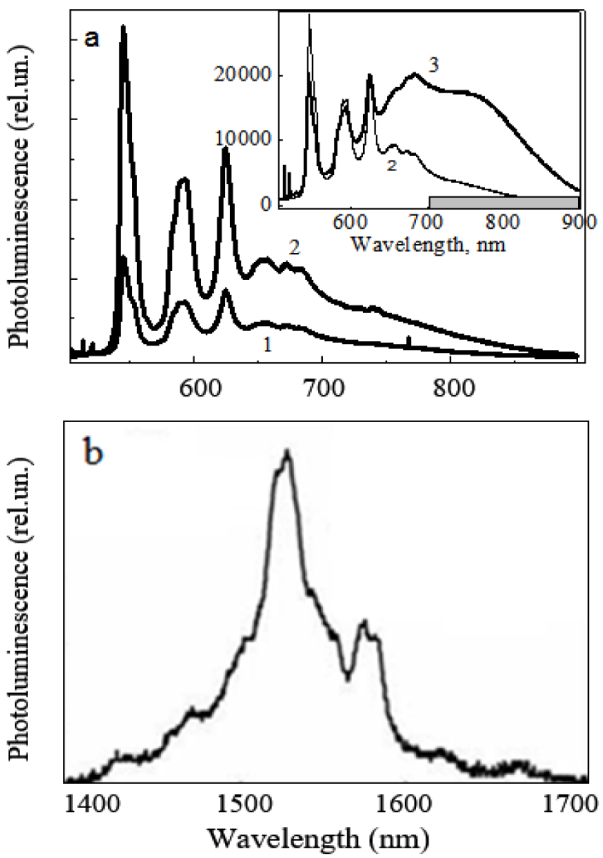

Figure 2. PL spectra of cBN:Tb micropowders with different Tb content (1—0.05, 2—0.1 at.% Tb) and in the inset—before (2) and after (3) annealing at T_{ann} = 870 K, λ_{exc} = 488 nm (a); PL spectrum of BN: Er micropowder, λ_{exc} = 960 nm (b); T_{reg} = 300 K.

cBN:Tb is characterized with appearance of broad band in range of 700-900 nm (the gray strip in **Figure 1(d)** and in the inset to **Figure 2(a))** of the multi-vacancy nature [5]. The PL spectrum in range of 1400-1700 nm of the cBN:Er single phase micropowder (0.05 at. % Er) is originated from the $^4I_{13/2} \rightarrow {}^4I_{11/2}$ electronic transitions (under the laser diode excitation with λ_{exc} = 960 nm) of the Er^{3+}ions incorporated into cBN crystal lattice (**Figure 2(b)**). The PL spectra of the cBN:Nd micropowders reflects the two-center character of Nd^{3+} ions in cBN, referring to our work [6]. The cBN:Sm micropowders under PL analysis are described by us in [7].

3.2. XRD Analysis of cBN:RE Micropowders

XRD patterns of cBN:RE micropowders showed their single phase nature, because the patterns contained only (111), (200), (220), (311) and (331) peaks which belonged to cBN with the face-centered cubic lattice (FCC). We will not pay attention here to features of the patterns which were previously discovered by us from the comparative analysis of XRD patterns of cBN:RE and cBN standard. The features testify to the formation of disordered solid solutions of rare earth elements (Tm, Tb, Eu, Ce) on cBN basis [8]. In the present paper via analysis of shapes of peaks in XRD patterns of cBN:RE, we develop our conceptions about a possible distortions of the cBN rigid crystal lattice, which can be caused by impurities of large sizes (the RE^{3+} ions here) of various concentrations. Peaks (111), (220), and (311) in XRD patterns of cBN:RE (in particular of cBN:Eu, cBN:Nd) with the RE smallest concentrations and the RE largest concentrations are represented in **Figure 3** and **Figure 4**. Hereinafter, a content in weight percent of any RE compound within a total mass of the precursor, is specified in parentheses next to the content in atomic percent. As seen from **Figure 3** and **Figure 4** when the concentration of Eu and Nd in cBN increases from less than ~0.01 at.% (0.5; 1) up to ~0.05 at.% (10), the peaks are decreased in intensity. With the concentration increasing, peaks (111), (220), (311) and (331) are displaced to the low 2Θ range, testi fying to the disordered solid solutions' creation. We can refer to [8] as well.

As established, all peaks in XRD patterns of all cBN:RE micropowders are variously asymmetric. Mainly, because the low 2Θ-branches of peaks (111), (220) and (311) are enormously stretched towards the low 2Θ-angles, particularly, for cBN with the RE

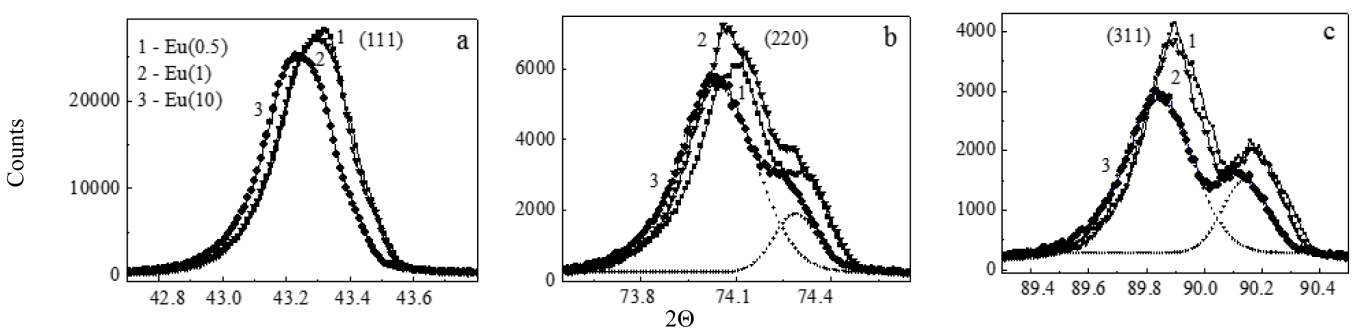

Figure 3. Peaks (111) (a); (220) (b); (311) (c) in XRD patterns of the cBN:Eu micropowder with the Eu different content in cBN: 1, 2 - < 0.01 at.% (0.5; 1), 3 - ~0.05 at.% (10); peaks 3 (b, c) approximated with two Gaussians, which are not $\acute{\alpha}_1$-$\acute{\alpha}_2$- -doublets.

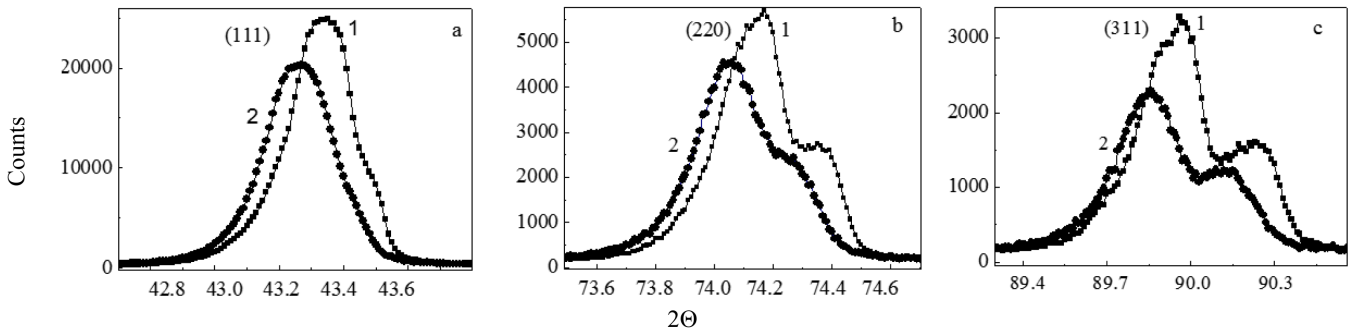

Figure 4. Peaks (111) (a); (220) (b); (311) (c) in XRD patterns of cBN:Nd micropowder with the Nd different content in cBN: 1 - < 0.01 at.% (1), 2 - ~0.05 at.% (10).

smallest content (less than 0.01 at.%). This effect is less expressive for cBN with the RE largest content, testifying to the noninstrumental nature of the asymmetry. It is known, that Guassians, Lorenzians and Voigtians are symmetric.

As seen in **Figures 3(b)** and **Figures 3(c)** and **Figure 4(b)** and **Figures 4(c)**, the asymmetric peaks (220) and (311) are finely structured. This allows to suggest that XRD patterns of cBN:RE contain the extra-peaks which are split from the parent peaks of cBN. When the RE concentrations in cBN increase (the peak 3 in **Figure 3**, the peak 2 in **Figure 4**), the peaks (220) and (311) change their profiles for smoothed shape and at first look loose the fine structure. However, if to decompose the peaks 3 and 2 into two Gaussians (dotted lines) or two Voigtians (not represented), the obtained doublets will not satisfy the requirements to $Cu_{K\acute{a}}$-doublet neither in intensities of their components nor in their widths. The same is related to peaks (111) and (331). Two Lorenzians absolutely are not acceptable in all cases. Thus, like the results on cBN:RE with the RE smallest concentration, the peaks of XRD patterns of the cBN:RE with the large RE concentration also possess the more complicated structure than single $Cu_{K\acute{a}}$-doublets.

It is known that a small deviation from cubic symmetry of crystal lattice leads to its distortions of different types. The perfect lattice (primitive cubic, BCC, FCC) possess the singlet lines (peaks) in its XRD pattern at the use of synchrotron monochromatic irradiation. Under the polychromatic $Cu_{K\acute{a}}$-irradiation, all lines in the XRD pattern should be represented with $Cu_{K\acute{a}}$-doublets. The singlet lines (otherwise, α_1- and α_2-component of $Cu_{\acute{a}}$-doublets) are characterized with multiplicity factor *m* which is the number of reflections which superimpose in the same diffraction peak and cannot be resolved in a perfect crystal lattice, satisfying the rule for the multiplicity factor *m*. If cubic crystal lattice is distorted, additional peaks appear in the "subcubic" XRD pattern, which are split from basic peaks in XRD pattern of the parent cubic crystal lattice, breaking the rule for the *m* factor. If to analyze the splitting scheme of the basic peaks, it is possible to define the type (tetragonal, trigonal and so on) of the distortions of cubic crystal lattice [9]-[11]. If the parent primitive or body centered or face centered cells of cubic crystal lattices are distorted, three different splitting schemes of basic peaks of the parent XRD patterns should be realized. In our mind, these schemes are not widely described in literature and we would refer the readers to [12] [13]. Worthy to add, that

the mentioned splitting schemes are realized when all cells of a cubic crystal are uniformly distorted. The type of distortion of the FCC crystal lattice of cBN could be revealed when the number of extra-splits around each parent peak of XRD pattern of the material was known. The characteristics (relative integral intensity and angular distance from the corresponding parent peak) of the extra-splits allow to estimate the distortion quantitatively as well as to suggest a way of its creation. The relative integral intensity is directly connected with the part of the crystallographic planes from the multiplicity {hkl} which don't participate in formation of the (hkl) basic peak. The angular distance allows to evaluate *e.g.* the quantitative characteristics of tetragonal and trigonal distortions Δa and $\Delta\gamma$ where a is the parameter of cubic cell and γ is the basic angle of the cell.

In this work, peaks (111), (220), (311) of XRD patterns of all micropowders cBN:RE were deconvoluted into Voigtians. The extra-splits (as the additional ones to peaks of the parent cBN) were discovered and compared in their numbers and characteristics in dependence on the RE concentration in cBN and on sizes of the RE^{3+} ions. In correspondence with atomic numbers in the periodic table, the sizes of the RE three-charged ions should increase in the series Er^{3+}, Tb^{3+}, Eu^{3+}, Sm^{3+}, Nd^{3+}. Any two lines resulted from the deconvolution were assigned with $Cu_{K\acute{a}}$-doublets if additionally to the features which were mentioned above, they possessed the similar contributions of Gaussians and Lorentzians. Making the suggestion about nonresolved $Cu_{K\acute{a}}$-doublets (broad peaks) as result of the deconvolution, we also kept in mind that a sum of two Voigtians is a Voigtian as well.

Being in shortage of the paper space, we represent the characteristic XRD patterns of cBN:RE with different doping levels. **Figure 5** particularly shows the deconvoluted peaks (111), (220) and (311) in XRD patterns of cBN:Er (5) and cBN:Nd (1) (less than 0.01 at. % RE in cBN). **Figure 6** particularly shows the peaks in XRD patterns of cBN:Tb (12) and cBN:Sm (10) with ~0.05 at. % RE. The deconvolution is represented for the cBN:Er (20) micropowder with the RE content above 0.1 at.% (**Figure 7**). As seen from **Figure 5**, the cBN parent peaks (111), (220) and (311) are accompanied with extra-splits at the low 2Θ-position and the high 2Θ-position. When the RE concentration increased up to ~0.05 at. % RE, the parent peaks (220) and (311) lost the neighbors on the right. The extra-splits at the high 2Θ-position follow only the (111) basic peaks but lost in intensity (compare **Figure 6** with **Figure 5**). The similarly organized XRD patterns of the cBN:Er are just redistributed in intensity (compare **Figure 7** with **Figure 6**). As seen, the intense basic peaks of cBN are there in all XRD patterns of cBN:RE confirming the presence of the cBN parent cells. It should be reminded, that the extra-splits at the low 2Θ and the high 2Θ arise from the planes within multiplicity {hkl}, correspondingly, with the enlarged and the diminished interplanar distances, which appear in crystal lattice of cBN due to the RE ions' incorporation. In case, the enlarged interplanar distances d_{hkl} in the cBN crystal lattice, appear due to large sizes of doping impurities. Possibly, that the diminished interplanar distances in the cBN crystal lattice can appear due to vacancies' creation which have to play the role of the mechanical strains' relaxants as well as compensators of the RE^{3+} ions' electrical charge.

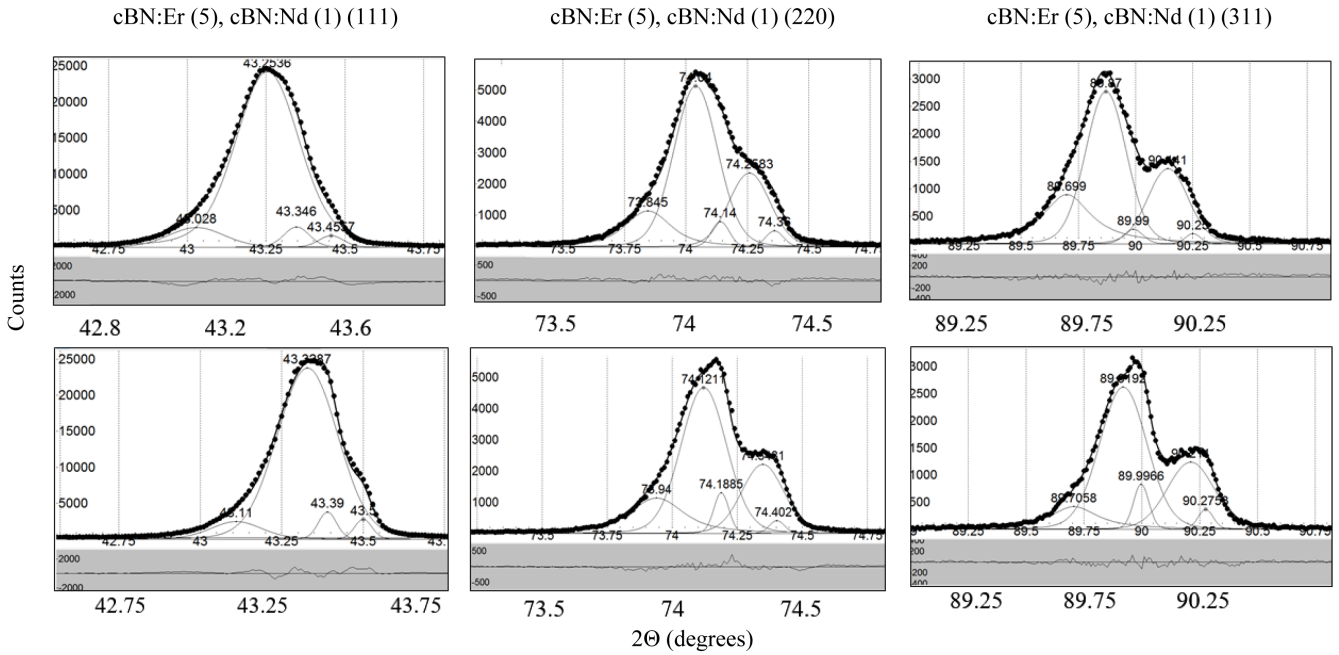

Figure 5. Peaks (111), (220) and (311) in XRD patterns of cBN:Er (5), cBN:Eu (2) and cBN:Nd (1) micropowders with the RE content less than 0.01 at.%, deconvoluted into Voigtians which are the resolved and nonresolved $Cu_{K\acute{a}}$-doublets.

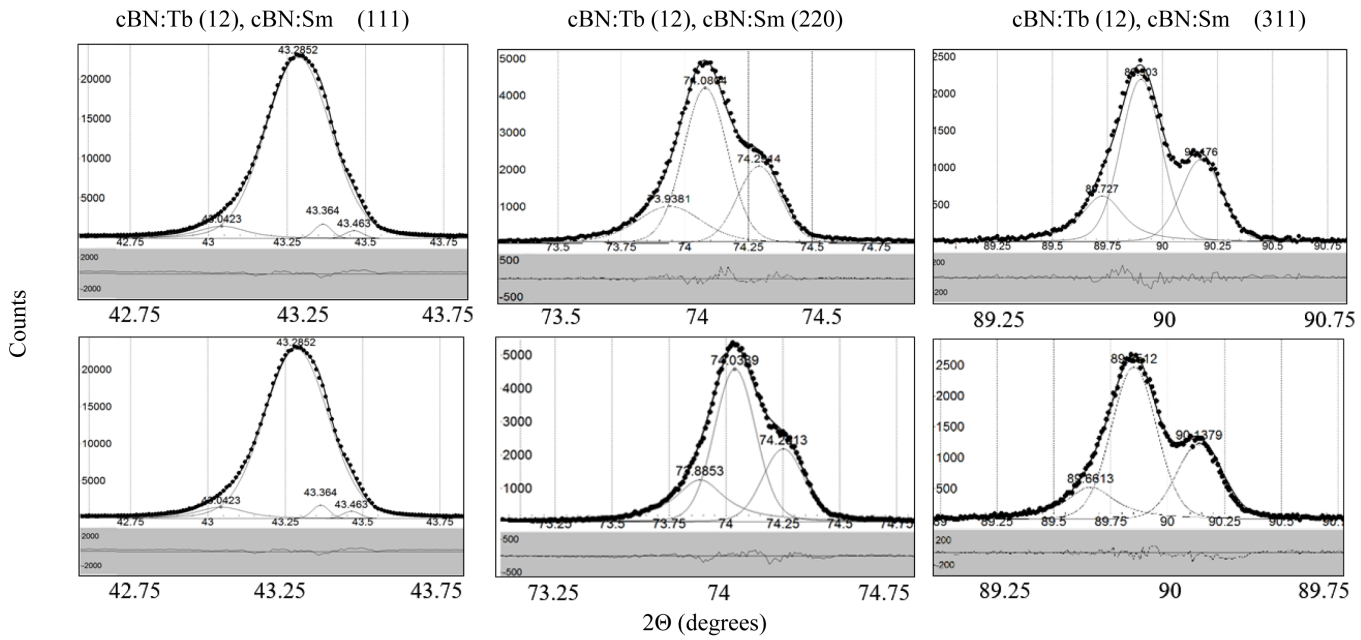

Figure 6. Peaks (111), (220) and (311) in XRD patterns of cBN:Eu (10), cBN:Tb (12) and cBN:Nd (10) micropowders with the RE content of ~0.05 at.%, deconvoluted into Voigtians which are the resolved and nonresolved $Cu_{K\acute{a}}$-doublets.

It seems, that we have managed to reveal some regularities and tendencies in behavior of XRD patterns of cBN which is doped with impurities of large sizes. It means that we can foresee a state of the cBN crystal lattice and realize the doping control of cBN within the investigated concentrations and errors of the deconvolutions.

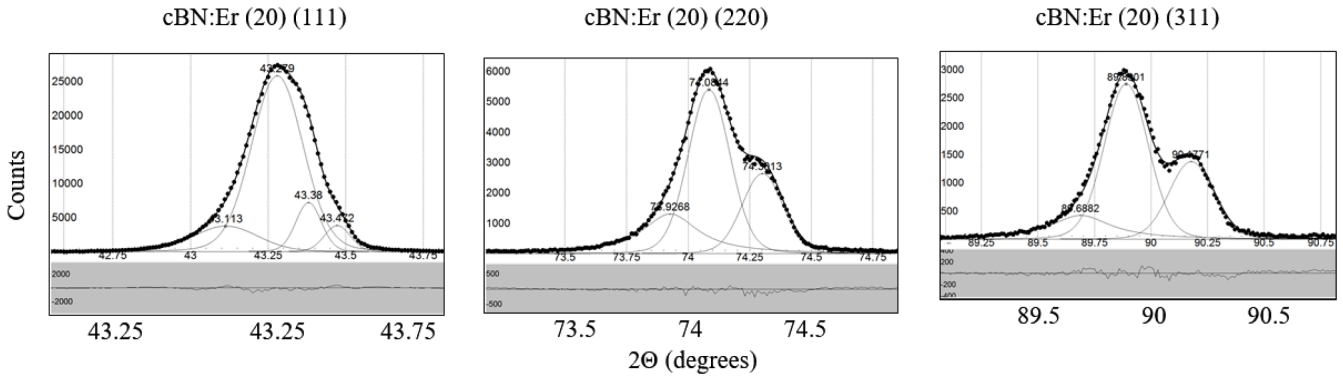

Figure 7. Peaks (111), (220) and (311) in XRD patterns of cBN:Er (20) and cBN:Tb (17) micropowders with content of Er and Tb in cBN above 0.1 at.% are deconvoluted into Voigtians, which represent the resolved and nonresolved CuKά-doublets.

As the evaluation criteria for the latter, we selected the main characteristics of the extra-splits in XRD patterns of cBN:RE: their fixed number around each parent peak of cBN, relative integral intensity and angular distance from the corresponding parent peak.

The number of extra-splits is clearly seen from **Figures 5**-**7**. The remaining characteristics can be analyzed from **Figures 8(a)-(b')** where they are mediately represented in dependence on the RE^{3+} ions' sizes and their concentrations in cBN. The number of narrow extra-splits around the parent peaks (111), (220) and (311) in XRD pattern in **Figure 5** cannot satisfy any splitting schemes [12] [13]. Thus, they only prove the nonuniformly distorted state of the cBN:RE crystal lattice with the small RE concentration. This state changes simultaneously with the RE concentration growth, but it doesn't reach the uniformity within the RE concentrations in cBN which were used here. Formally, we got that the splitting schemes could not be applied neither to the small concentrations nor to any concentrations of the RE in cBN which are investigated in the present work. Thus, the crystal lattice of cBN:RE represents the disordered solid solution which is nonuniformly distorted. To draw conclusions, we accept that the extra-splits are resulted from the RE ions' invasion of the {hkl} planes.

The dependences in **Figure 8** let us reveal some suggestions about a possible mechanism of redistribution of the RE^{3+} ions inside the cBN crystal lattice. In cBN:RE with the equal concentration of different REs, the larger is the RE ion's size, the more number of (111) planes are occupied or "attacked" by the ions (**Figure 8(a)**); the planes (220) can be occupied by all ions except the largest ones. With the growth of the RE ion's size the planes (311) can be well occupied by the smallest ions (Er^{3+} and Tb^{3+}), and less with the Sm^{3+} ions and much less by the Nd^{3+} largest ions. From **Figure 8(a)** and **Figure 8(b)** follows, the more number of planes {hkl} are affected by the ions, the smaller the interplanar distances between the planes which give rise to the extra-splits around the cBN parent peaks in XRD patterns of cBN:RE. The RE^{3+} ions of one sort preferably try to occupy the planes {220} and {311} from all available planes {hkl} in crystal lattice of cBN, except the Nd^{3+} ions which go into {220)} panes.

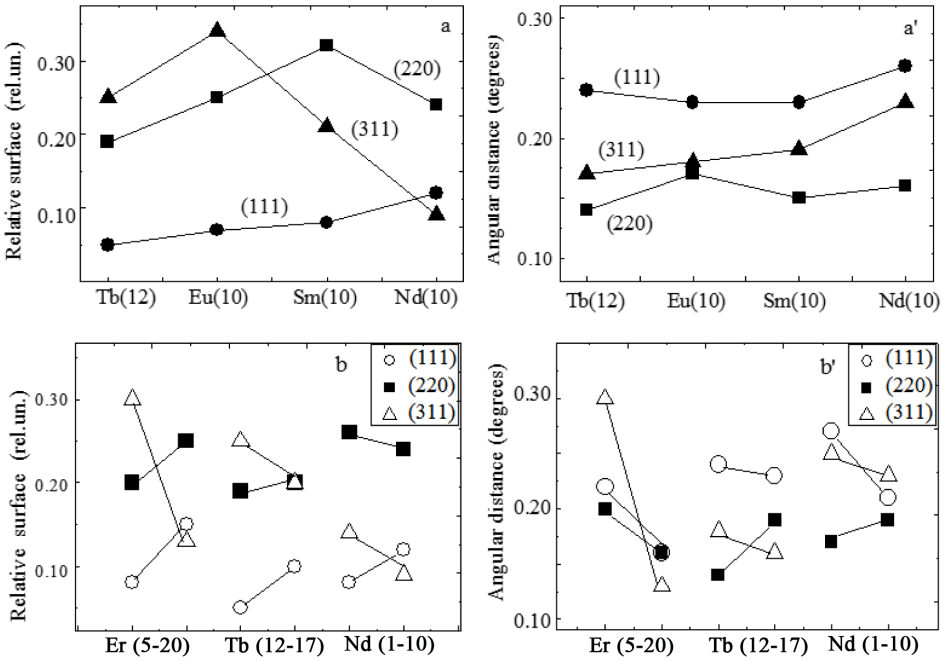

Figure 8. Dependences of the relative surface of the low 2Θ extra-split and of the angular distance between maximum of the extra-split and the corresponding basic peak (shown near the plots) in XRD patterns of cBN:RE micropowders with the similar RE concentration, on the RE^{3+} radius in the series Er^{3+}, Eu^{3+}, Sm^{3+}, Nd^{3+} (a, a'); and on the concentration of the same RE ions in cBN (b, b'). Concentrations of the RE compound within the total mass of the precursors of the cBN:RE micropowders, are shown in parentheses.

As seen from **Figures 8(a')** and **Figure 8(b')**, when the concentration of the RE in the cBN:RE increases, the larger number of planes {111} and the smaller number of planes {311} can be affected by all RE ions and the larger number of planes {220} will be affected by all except the Nd^{3+} largest ions. When the concentration of the RE in the cBN:RE increases, the larger number of the planes {111} and the smaller number of planes {311} with diminishing distances between the planes can be created in cBN, which give rise to the extra-splits formation. Simultaneously, the number of the planes {220} and the interplanar distances between, which give rise to the extra-splits, can vary in dependence on the RE concentration in cBN and on the ions' size. However, at average, the different RE ions affect the larger number of planes (220) as to compare to planes (111) and (311) when concentration of the RE in cBN increases (**Figure 8(a')**).

4. Conclusions

The light emitting cubic boron nitride doped with rare earth elements (cBN:RE) in form of micropowders with the RE content in cBN from less than 0.01 up to more than 0.1 at.%, is synthesized, tested in IR-, red and green photoluminescence and precisely investigated using XRD analysis. New data conclusively testify Eu^{3+} ions to occupy two sites of low symmetry in cBN crystal lattice and to create two luminescence centers (Eu1 and Eu2). The Eu^{3+} ions occupy the second site in cBN crystal lattice the more ex-

pectable, the more concentration of Eu in cBN. The Tb^{3+} ions don't change the single position in cBN crystal lattice with the concentration growth as well as after similar annealing which leads the Eu^{3+} ions to multiply their positions and the luminescence centers in cBN up to four. With high probability, the intrinsic atoms of boron and nitrogen in the tetrahedral symmetry's positions can be substituted by the Tb^{3+} ions, because these positions are most stable and energy-optimal. It is logically to expect the smallest RE^{3+} ions to occupy the similar positions, and the RE^{3+}largest ions to have two or more crystallographic positions of low symmetry in crystal lattice of cBN. The latter is well supported with our previous results on cBN:Nd, cBN:Gd and cBN:Ce.

All cBN:RE micropowders (RE: Er, Tb, Eu, Sm, Nd) showed the cBN single phase content under XRD analysis. In XRD patterns of cBN:RE, as the whole, the angular displacements of peaks to the low 2Θ positions with the RE concentration growth, did not follow the rule for the ordered solid solutions, the Bragg angle increases, the shift is the strong. This testifies to the creation of disordered solid solutions of the RE on cBN basis.

As established, all peaks in XRD patterns of cBN:RE were variously asymmetric with the asymmetry of noninstrumental nature. In consideration of the latter and the peaks' shape analysis, the narrow extra-splits around the cBN parent peaks were revealed and analyzed in dependence on the RE^{3+} ions' size and the RE concentrations in cBN. As shown, the extra-splits' formation is subject to the regularities. On their basis, some suggestions are made about a possible mechanism of redistribution of the RE^{3+} ions inside the cBN crystal lattice.

The extra-splits' appearance in XRD patterns of the cBN:RE micropowders, and their regular transformations simultaneously with the cBN parent peaks' angular displacements, allow to assume that the RE large ions as create disordered solid solutions on the cBN basis, as bring some cells of the cBN parent crystal lattice to distorted states and their changes. Still, these states stay out of the classical uniform distortions of cubic crystal lattices (tetragonal, trigonal *e.g*). From characteristics of the extra-splits, the cBN crystal lattice is not seriously deteriorated in the investigated span of the RE concentrations. We expect new data to define a possible limit for concentrations of large impurities in cBN which start to break the cBN crystallographic identity.

Acknowledgements

E. Sh. thanks J. W Steeds (PL) and V. G. Luhin (XRD) for the measurements' providing. Without very precise PL and XRD records the work would be impossible.

References

[1] Abtew, T.A., Gao, W.W., Gao, X., Sun, Y.Y., Zhang, S.B. and Zhang, P.H. (2014) Theory of Oxygen-Boron Vacancy Defect in Cubic Boron Nitride: A Diamond NV-Isoelectronic Center. *Phys. Rev. Let.*, **113**, 134401.

[2] Gaiduk, M.I., Zolin, V.F. and Gaigerova, L.S. (1974) The Luminescence Spectra of Europium. Nauka, Moscow.

[3] Shishonok, E.M., Leonchik, S.V., Braud, A., Steeds, J.W., Abdullaev, O.R., Yakunin, A.S.

and Zhigunov, D.M. (2010) Photolu-Minescence of Micropowders of Europium-Doped Cubic Boron Nitride. *J. Opt. Technology*, **77**, 788-795.

[4] Shishonok, E.M. (1990) Study of the Defect-Formation Processes in Cubic Boron Nitride Using Optical Methods. Dissertation for Candidate of Physicomathematical Sciences, Minsk.

[5] Shishonok, E.M. (2009) Cubic Boron Nitride: Raman and Luminescence Investigations, Prospects for Use in Opto- and Microelectronics. Publ. Center of Belarussian State University, Minsk.

[6] Shishonok, E.M., Leonchik, S.V., Bodiou, L. and Braud, A. (2009) Photoluminescence Investigations of Cubic Boron Nitride Doped with Neodymium during High-Pressure Synthesis. *Physics of the Solid State*, **51**, 1828-1835.

[7] Shishonok, E.M., Leonchik, S.V. and Steeds, J.W. (2008) Luminescence of Samarium-Activated cubic Boron Nitride. *J. Applied Spectroscopy*, **75**, 89-95.

[8] Shishonok, E.M., Steeds, J.W., Pysk, A.V., Mosunov, E.O., Abdullaev, O.R., Yakunin, A.S. and Zhigunov, D.M. (2012) Structural Studies of Rare-Earth Activated Cubic Boron Nitride Micropowders. *Powder Metallurgy and Metal Ceramics*, **50**, 754-767. http://www.springerlink.com/openurl.asp?genre=article&id=doi:10.1007/s11106-012-9386-5 http://dx.doi.org/10.1007/s11106-012-9386-5

[9] Darul, J. (2009) Thermal Instability of the Tetragonally Distorted Structure of Copper-Iron Materials. Z. *Kristallogr. Suppl.*, **30**, 335-340.

[10] Lindbaum, A., Heathman, S., Le Bihan, T. and Rogl, P. (2000) Pressure-Induced Orthorhombic Distortion of UMn_2. *J. Al loys & Compounds*, **298**, 177-180. http://dx.doi.org/10.1016/S0925-8388(99)00627-1

[11] Le Bihan, T., Idiri, M. and Heathman, S. (2003) New Investigation of Pressure-Induced Rhombohedral Distortion of Uranium Nitride. *J. Alloys & Compounds*, **358**, 120-125. http://dx.doi.org/10.1016/S0925-8388(03)00078-1

[12] Abakumov, A.M. www.emat.ua.ac.be/xel2006/course%20material/X-2006CD/Abakumov/LectureAbakumov.doc

[13] Weaver, M.L. http://bama.ua.edu/~mweaver/courses/MTE583/MTE%20583_Class_17.pdf